SIMULATION OF THE FRICTION FACTOR IN A YIELD-STRESS SLURRY FLOW WHICH EXHIBITS TURBULENCE DAMPING NEAR THE PIPE WALL

Artur Bartosik

Kielce University of Technology, Chair of Engineering Production, Kielce, Poland

e-mail: artur.bartosik@tu.kielce.pl

The paper deals with the mathematical modelling of fully developed turbulent flow of a Bingham hydromixture in a pipe. The mathematical model is based on time averaged Navier-Stokes equations and uses the apparent viscosity concept. The problem of closure of the turbulence stress tensor was solved by the two-equation turbulence model in which a modified turbulence damping function was taken into account. The final form of the mathematical model constitutes a set of three non-linear partial differential equations. The main aim of the paper is to demonstrate a significant decrease of turbulence near the pipe wall, as the friction factor is below that for a water flow. The paper presents results of numerical simulation of the frictional head loss and friction factor for slurry flows with low, moderate, and high yield stresses. Predicted frictional head losses have been compared with experimental data showing satisfying agreement. It is demonstrated that the frictional head loss and the friction factor substantially depend on the yield stress. The results of numerical simulation are presented as figures and conclusions. Possible causes of turbulence damping near the pipe wall are discussed.

Key words: Bingham flow, turbulence modelling, damping of turbulence, friction factor simulation

Nomenclature

C_i – constant in Lauder and Sharma turbulence model, $i = 1, 2$

d_p – solid particle diameter [μm]

D – inner pipe diameter [m]

f_μ – turbulence damping function at pipe wall

I – intensity of turbulence

k – kinetic energy of turbulence [m^2/s^2]

MDF – modified turbulence damping function, (3.13)

p – static pressure [Pa]

r – distance from symmetry axis [m]

R^+ – dimensionless distance from pipe wall

$\mathrm{Re}_t, \mathrm{Re}_{ap}$ – turbulent Reynolds number and Reynolds number for apparent viscosity, respectively

SDF – standard turbulence damping function, (3.14)

t^* – relaxation time of solid particle [s]

T – temperature [K]

U, V – velocity component in ox and or direction, respectively [m/s]

u', v' – fluctuating components of velocity U and V [m/s]

x, y – coordinate for ox direction and distance from the pipe wall, respectively [m]

$\overline{(\cdot)}$ – time averaged

Greek symbols

γ – strain rate [s^{-1}]

ε – rate of dissipation of kinetic energy of turbulence [m^2/s^3]

λ – friction factor

μ, μ_{ap}, μ_{pl} – dynamic viscosity coefficient, apparent viscosity and plastic viscosity in Bingham rheological model, respectively [Pa·s]

ρ – density [kg/m^3]

σ_i – diffusion coefficients in k-ε turbulence model, $i = k, \varepsilon$

τ, τ_0, τ_w – shear stress, yield and wall shear stress, respectively [Pa]

Indexes

ap – apparent, b – bulk (cross-section averaged value), l – liquid, m – slurry (solid-liquid mixture), p – particle (solid phase), t – turbulent, w – solid wall.

1. Introduction

The solid-liquid flow is widely employed in the mining and chemical industries in slurry pipelines (Shook and Roco, 1991). The solid-liquid flow can include those dealing with composite materials, rocks, rubber, pharmaceuticals,

biological fluids, plastics, petroleum, cement, food products and paper pulp. There is an increasing demand to create slurred minerals at the mining faces to be transported to the processing plant and the subsequent recycling of the waste from the plant to the tailings dam or to mined out areas as a backfill. As an example, Black Mesa pipeline transports partially-processed coal slurry from the mine to a power plant more than 430 km distance. The horizontal pipe diameter is 0.457 m while the downward pipe diameter is 0.254 m. Recent decades have seen a great increase in the transport of waste materials in the slurry form, to suitable deposit sites.

Compared with the conventional transportation of solids, the slurry pipe flow has several advantages, such as its friendliness to the environment and its relatively low operation and maintenance costs. It has been the endeavor of researchers around the world to develop accurate models to predict pressure drop in slurry pipelines, as the pressure drop is the crucial parameter which dictates the selection of pump capacity.

The paper deals with the turbulent flow of solid-liquid mixture in a pipe. The carrier liquid phase is water while solid particles are fine with median particles diameter between 5 and $30\,\mu$m. The flow is steady, fully developed, homogeneous and axially symmetrical. Rheological properties of a slurry flow exhibit non-Newtonian behaviour, and the dependence of the shear rate on the shear stress is approximated using Bingham's model. A single-phase continuum model, proposed by Bartosik (1997), is explored to calculate friction factor in such a turbulent slurry flow. The mathematical model is based on time-averaged Navier-Stokes equations. The problem of closure of the turbulence stress tensor is solved by the k-ε turbulence model in which the modified turbulence damping function is taken into account (Bartosik, 1997). The mathematical model uses the apparent viscosity concept and the apparent viscosity is calculated with the application of Bingham's rheological model. Finally, the mathematical model constitutes a set of three partial differential equations, namely momentum, kinetic energy of turbulence, rate of dissipation of kinetic energy of turbulence and complimentary algebraic equations including the modified turbulence damping function.

The paper presents results of numerical simulation of the frictional head loss and friction factor for various slurry flows with low, moderate, and high yield stresses.

The main aim of the paper is to demonstrate the significant decrease of turbulence near the pipe wall, as the friction factor is below that for a water flow, which is especially seen for Reynolds numbers below $100\,000$.

2. Literature review

Determining the most efficient and economical way of pumping any solids with carrier liquid requires careful consideration and analysis of numerous factors. Some of them can have a significant impact on the performance and costs. Among them, there is a constitutive relation between stress and deformation, particle diameter, solid concentration, particle and liquid density, deposition velocity, and properly matched characteristics of the pipeline and the pump. For that reason, the solid-liquid turbulent flow belongs to main challenges of computational fluid dynamics and mixture theory models are the most general and based on rigorous fluid mechanics framework (Hinze, 1971; Soo, 1990).

All slurries can be broadly divided into two general groups of non-settling or settling types. Non-settling slurries contain very fine particles which can form stable homogeneous mixtures exhibiting an increased apparent viscosity, and in some cases, turbulence damping (Bartosik, 2010). Settling slurries are formed by coarse particles. The basic flow patterns observed in slurries of coarse particles are: stationary bed, moving bed, heterogeneous flow, and pseudo-homogeneous (Doron and Barnea, 1996).

Modification of turbulence by dispersed solid particles has been investigated experimentally by several researchers. The structure of turbulence in the near-wall region was examined by Kuboi *et al.* (1974), Schreck and Kleis (1993), Nouri and Whitelaw (1992), Chen and Kadambi (1995) for maximum possible solid concentration up to 25% by volume. It was shown that ejection-sweep cycle is affected strongly by particles, and the slip velocity decreases with increasing solid concentration. Generally, one can say that if the solid particles are sufficiently small, their relaxation time, defined by equation (2.1), is low, and they can follow the carrier fluid. In such a case, the diffusion process distributes particles uniformly across the stream. When coarse particles are considered, their relaxation time is high and additional particle-particle interactions and swirls or wakes appear causing the level of turbulence and resistance to be increased. The turbulence attenuation or generation can have enormous effects on costs of solids transportation, yet there is no theory or model that would give consistently accurate predictions of turbulence modification. The physical mechanisms are also so poorly understood that experts in the field cannot predict if turbulence attenuation or generation will occur in a given flow

$$t^* = \frac{d_p^2 \rho_p}{18\mu_l} \tag{2.1}$$

A number of scientific challenges which represent building blocks for the comprehensive understanding of disperse flows encountered in a variety of technologies and in nature was outlined by Sundaresan *et al.* (2003). They concluded that new experiments and analyses are needed to cast light on the important phenomena that cause turbulence attenuation or generation. The authors suggested that the experiments should be conducted in simple turbulent flows such as fully developed pipe or channel flow, or simple axisymmetrical flows. Regardless of geometry, the experiments must include a wide range of particle parameters (mainly size and density) in a single fixed facility.

Among turbulence models dedicated to the slurry flow with fine particles, one can take into account a one-equation turbulence model by Danon *et al.* (1997), Roco and Shook (1983), Roco and Balakrishnan (1985), Wu (1996), Li and Zhou (1996), Mishra *et al.* (1998) or two-equation k-ε-Ap model of Yulin (1996) and Ling *et al.* (2003). As an example, Danon *et al.* (1997), built a one-equation $k - l$ turbulence model using an empirical turbulence length scale. The two-equation k-ε-Ap turbulence model by Yulin (1996), in which k and ε are kinetic energy of turbulence and its dissipation rate, respectively, is the same like in the standard turbulence model for a single phase flow. The Ap is an algebraic equation describing the solid phase. The mathematical model was successfully examined but for low values of solids concentration.

Stainsby and Chilton (1994, 1996) developed a hybrid model in which the apparent viscosity was calculated by the Herschel-Bulkley rheological model at a low strain rate and by the Bingham model at a high strain rate. Using the time-averaged momentum equation and low Reynolds numbers, the k-ε model by Launder and Sharma (1974) could predict the pressure drop and velocity distribution in a fine-dispersive slurry flow. The authors did not include any changes in the k-ε turbulence model. They emphasized that the related error of pressure drop prediction using their mathematical model is less than 15%. However, it must be noted that their hybrid model was successfully examined only for low solids concentrations and low yield stresses, and the maximum slurry density was $1105 \, \text{kg/m}^3$.

Cui and Grace (2007) made a literature review on newest experiments and modelling of solid-liquid flows with special attention to paper pulp. They noted progress in techniques of determining fiber flocculation and laminar-turbulent transition. They noted that new models based on Computational Fluid Dynamics appeared, however their potential was limited by lack of properly defined suppression and/or amplification of turbulence and solid-liquid interactions.

Slurries with fine-particles usually exhibit yielding behaviour and are referred to as viscoplastic or yield-stress liquids, (Shook and Roco, 1991). This

is quite common that such slurries exhibit damping of turbulence, (Wilson and Thomas, 1985; Bartosik, 2008). As it was mentioned above, in the case of limited access to reliable experimental data of turbulence at close vicinity of the pipe wall over a wide range of solids concentrations, it is difficult to suggest appropriate turbulence models for the slurry flow. However, it is possible to suggest a modification to the existing turbulence models on the basis of comparison between calculations and measurements of global parameters, such as frictional head loss and velocity profile. These quantities are very important for proper designing of pipeline characteristics, pump impellers, and for proper calculation of heat transfer processes.

3.   Mathematical model

The physical model assumes that the flow constitutes water and fine solid particles with median diameter between 5 and 30 μm. The flow is steady, fully developed with sufficiently high bulk velocity that the flow can be assumed as homogeneous, and axially symmetrical. Rheological properties of a slurry flow exhibit non-Newtonian behaviour and the dependence between shear stress and shear rate can be approximated by Bingham's model (Bartosik, 1997; Bartosik *et al.*, 1997).

Taking into account a Newtonian fully developed and axially symmetrical pipe flow, the final form of the time-averaged momentum equation can be described, as follows

$$\frac{1}{r}\frac{\partial}{\partial r}\Big[r\Big(\mu\frac{\partial \overline{U}}{\partial r} - \overline{\rho u'v'}\Big)\Big] = \frac{\partial \overline{p}}{\partial x} \tag{3.1}$$

in which the turbulent stress tensor was found by making use of the Boussinesque hypothesis, as follows

$$-\rho\overline{u'v'} = \mu_t\frac{\partial \overline{U}}{\partial r} \tag{3.2}$$

and the turbulent viscosity was determined through dimensionless analysis, and equals

$$\mu_t = f_\mu\frac{\overline{\rho}k^2}{\varepsilon} \tag{3.3}$$

The k and ε were calculated using the Launder and Sharma turbulence model (Launder and Sharma, 1974) according to:

— the equation for kinetic energy of turbulence

$$\frac{1}{r}\left[r\left(\mu + \frac{\mu_t}{\sigma_k}\right)\frac{\partial k}{\partial r}\right] + \mu_t\left(\frac{\partial \overline{U}}{\partial r}\right)^2 = \rho\varepsilon + 2\mu\left(\frac{\partial k^{1/2}}{\partial r}\right)^2 \qquad (3.4)$$

– the equation for dissipation rate of kinetic energy of turbulence

$$\frac{1}{r}\left[r\left(\mu + \frac{\mu_t}{\sigma_\varepsilon}\right)\frac{\partial \varepsilon}{\partial r}\right] + C_1\frac{\varepsilon}{k}\mu_t\left(\frac{\partial \overline{U}}{\partial r}\right)^2 = C_2\left[1 - 0.3\exp\left(-\mathrm{Re}_t^2\right)\right]\frac{\rho\varepsilon^2}{k} - 2\nu\mu_t\left(\frac{\partial^2 \overline{U}}{\partial r^2}\right)^2 \qquad (3.5)$$

in which the turbulent Reynolds number was defined using dimensionless analysis as

$$\mathrm{Re}_t = \frac{\overline{\rho}k^2}{\mu\varepsilon} \qquad (3.6)$$

Taking into account a non-Newtonian solid-liquid flow with fine particles, it is quite common that such slurries possess the yield stress. Viscoelastic fluid mechanics is the study of motions in which the kinematics can not be established *a priori*, and the continuity and momentum equations must be solved together with the constitutive equation, which includes the stress. Taking into account the Bingham rheological model, defined as

$$\tau = \tau_0 + \mu_{pl}\gamma \qquad \text{for} \qquad \tau > \tau_0 \qquad (3.7)$$

and

$$\gamma = 0 \qquad \text{for} \qquad \tau \leqslant \tau_0 \qquad (3.8)$$

one can calculate the apparent viscosity, defined as

$$\tau = \mu_{ap}\gamma \qquad (3.9)$$

Comparing (3.7) and (3.9) for $\gamma > 0$, the apparent viscosity can be described as follows

$$\mu_{ap} = \frac{\mu_{pl}}{1 - \frac{\tau_0}{\tau}} \qquad (3.10)$$

Instead of the molecular viscosity μ and liquid density ρ that appear in equations (3.1), and (3.4)-(3.6), the apparent viscosity μ_{ap} and the slurry density ρ_m are used in the mathematical model. It must be noted however, that equation (3.10) has some limitation as the yield stress cannot be equal to or exceed the shear stress. Unfortunately, such situations can take place in close vicinity of the symmetry axis. This is due to the fact that the shear stress varies linearly from its maximum value at the pipe wall to zero in the symmetry axis. It means that at some distance from the symmetry axis the

shear stress can be lower than the yield stress. To avoid the situation where the shear stress can be lower or equal to the yield stress, it is assumed that the apparent viscosity is constant across the pipe and possesses the same value as at the pipe wall. For that reason, the final form of apparent viscosity, initially defined by (3.10), is calculated as

$$\mu_{ap} = \frac{\mu_{pl}}{1 - \frac{\tau_0}{\tau_w}} \qquad (3.11)$$

where the wall shear stress τ_w can be calculated from the balance of forces acting on the unit pipe length, as

$$\tau_w = \frac{dp}{dx}\frac{D}{4} \qquad (3.12)$$

The turbulence damping function f_μ, that appears in equation (3.3), called also the wall damping function, is an empirical function important in close vicinity of the pipe wall. The function has low values close to the pipe wall decreasing the turbulent viscosity and, in consequence, decreasing a component of the turbulent stress tensor described by equation (3.2), which is in accordance with measurements. For the fine-dispersive slurry flow with a yield stress, the wall damping function is determined on the basis of comparison between predictions and measurements (Bartosik, 1997), as follows

$$f_\mu = 0.09 \exp\left[\frac{-3.4\left(1 + \frac{\tau_0}{\tau_w}\right)}{\left(1 + \frac{\text{Re}_t}{50}\right)^2}\right] \qquad (3.13)$$

Turbulence damping function (3.13) has the dimensionless yield stress τ_0/τ_w and approaches the standard damping function, proposed by Launder and Sharma, as the yield stress approaches zero

$$f_\mu = 0.09 \exp\left[\frac{-3.4}{\left(1 + \frac{\text{Re}_t}{50}\right)^2}\right] \qquad (3.14)$$

However, with the yield stress increase in Eq. (3.13), at the same flow conditions $\tau_w = \text{const}$, the turbulence damping function decreases turbulent viscosity (3.3) and, in consequence, decreases turbulent shear stresses (3.2) at the pipe wall. This is coherent with the earlier observations of researchers who reasoned that in the fine-dispersive slurry the viscous sublayer becomes thicker, compared to a single-phase flow at the same flow conditions (Wilson and Thomas, 1985).

Finally, the mathematical model comprises three partial differential equations, namely (3.1), (3.4) and (3.5), together with complimentary equations (3.2), (3.3), (3.6), (3.13), and apparent viscosity (3.11) and wall shear stress (3.12). All numerical computations were made for known dp/dx values.

The mathematical model assumes non-slip velocity at the pipe wall, i.e. $U = 0$, and $k = 0$, $\varepsilon = 0$. Axially symmetrical conditions were applied at the pipe centre to all variables with $dU/dr = 0$, $dk/dr = 0$ and $d\varepsilon/dr = 0$. The turbulence constants in the model are the same as those in the Launder and Sharma model (Launder and Sharma, 1974): $C_1 = 1.44$; $C_2 = 1.92$; $\sigma_k = 1.0$; $\sigma_\varepsilon = 1.3$. The mathematical model was solved by a finite difference scheme using own computer code. Differential grid of 80 nodal points distributed across the pipe radius was used. Majority of the nodal points were localized near the pipe wall. The number of nodal points was set up experimentally to provide nodally independent predictions.

The mathematical model was examined for a comprehensive range of rheological parameters defined by Bingham, Casson, and Herschel-Bulkley models. Comparison of predictions of the frictional head loss and velocity distribution with measurements was successful, however an observable advantage of the Herschel-Bulkley rheological model compared to the Bingham and the Casson models was noted (Bartosik, 1997, 2001, 2006, 2010; Bartosik *et al.*, 1997). It must be emphasized, however, that the differences were not substantial (Bartosik, 2004, 2010).

4.   Simulation of the friction factor

All slurries taken into account are fine-dispersive with median particles diameter between 5 and 30 μm. The basic assumptions used in all the following predictions are that the Bingham rheological model is suitable for the slurry, and the mathematical model includes the modified turbulence damping function f_μ described by equation (3.13), which depends on the dimensionless yield stress τ_0/τ_w. Function (3.13) is different compared to that originally proposed by Launder and Sharma (1974), which is called here the standard damping function. The modified turbulence damping function f_μ, described by (3.13), increases damping of turbulence at the pipe wall much more compared to the standard damping function. In order to demonstrate the differences in prediction of frictional head loss and friction factor using both functions, namely: modified (3.13), denoted as MDF, and standard (3.14), denoted as SDF, both computations are presented in following figures.

Simulation of the slurry frictional head loss dp/dx and friction factor λ_m was performed for data collected in Table 1, which corresponds to real slurries with temperature $T = 298\,\mathrm{K}$.

Table 1. Parameters of slurries used for simulation

No.	τ_0 [Pa]	μ_{pl} [Pa·s]	ρ_m [kg/m³]	D [m]	Experiment
1	1.42	0.00301	1061.3	0.140	Slatter (1994)
2	4.92	0.00433	1105.3	0.790	Slatter (1994)
3	9.00	0.01300	1535.0	0.159	Bartosik *et al.* (1997)
4	13.50	0.02500	1335.0	0.263	Bartosik *et al.* (1997)
5	43.00	0.05000	1667.0	0.159	Bartosik *et al.* (1997)

As the Bingham rheological model is incorporated into the mathematical model, it should be noted that for a low yield stress the Bingham rheological model gives very good agreement of predictions with measurements over a comprehensive range of bulk velocities (Bartosik, 1997). For moderate and high yield stresses discrepancies exist. Prediction of the frictional head loss for a turbulent slurry flow with moderate yield stress, equal to $\tau_0 = 9\,\mathrm{Pa}$ and $\tau_0 = 13.5\,\mathrm{Pa}$, and for water are presented in Fig. 1 and Fig. 2, respectively. It is seen in Fig. 1 that for $\tau_0 = 9\,\mathrm{Pa}$ the predictions with modified (MDF) and standard (SDF) turbulence damping function are close to the experimental data. However, both predictions are different and the standard damping function (SDF) demonstrates higher, while the modified damping function (MDF) lower frictional head loss.
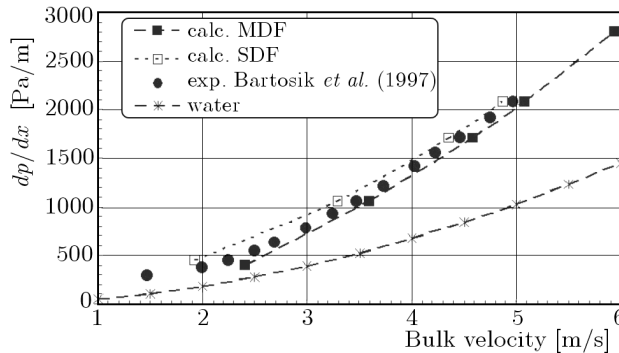

Fig. 1. Dependence of bulk velocity on frictional head loss of slurry flow using standard (SDF) and modified turbulence damping function (MDF); data No. 3 in Table 1

If the yield stress increases, the differences between predictions using standard (SDF) and modified turbulence damping function (MDF) increases too what is clearly seen in Fig. 2. It is demonstrated in Fig. 2 that predictions using SDF do not match experimental data, while predictions using MDF match them well. In both aforementioned Figures, the experimental data for the slurry flow are much higher compared to the water flow. Nevertheless, we expect higher values of the frictional head loss for the slurry flow than appears.
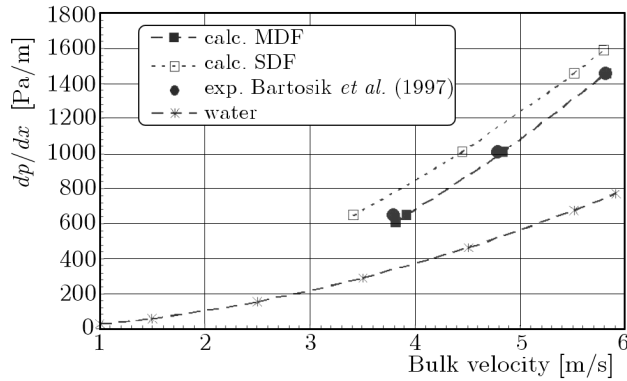

Fig. 2. Dependence of bulk velocity on frictional head loss of slurry flow using standard (SDF) and modified turbulence damping function (MDF); data No. 4 in Table 1

For a high yield stress, discrepancies between predictions using SDF and MDF are substantial. Taking into account the mathematical model together with the modified turbulence damping function gives good accuracy. This is demonstrated in Fig. 3, where the experimental data for laminar and turbulent slurry flow and the predictions using SDF and MDF are shown together with the experimental data for water flow.

The friction factor for a fine-dispersive slurry flow can be calculated from equation (4.1). The equation was developed from a simple balance of forces acting on a unit pipe length. The wall shear stress, appeared in (4.1), is designated by equation (3.12)

$$\lambda_m = \frac{8\tau_w}{\rho_m U_b^2} \qquad (4.1)$$

When the problem of friction factor λ is discussed, it is always questionable which Reynolds number should be taken into account as there are different approaches towards calculations of the Reynolds number. This is also important when determining laminar-turbulent transition. Comprehensive investigation of the present state of the art regarding the prediction of transition in a slurry flow with a yield stress and formulation of practical guidelines for design
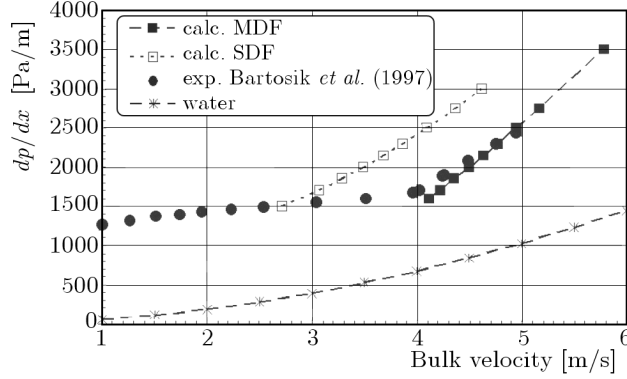
Fig. 3. Dependence of bulk velocity on frictional head loss of slurry flow using standard (SDF) and modified turbulence damping function (MDF); data No. 5 in Table 1

engineers, was done by Slatter and Wasp (2000). In the present study, the apparent viscosity concept, described by equation (3.11), has been used. For this reason, the Reynolds number is defined as

$$\mathrm{Re}_{ap} = \frac{\rho_m U_b D}{\mu_{ap}} \tag{4.2}$$

Simulation of the friction factor, described by equation (4.1), was performed for data set collected in Table 1, and is presented in Fig. 4. All predictions of λ_m for a fine-dispersive slurry flow using SDF are slightly below the data for water flow λ. However, taking into account MDF, the predictions of friction factor for slurry flows with low, moderate, and high yield stress, demonstrate significantly lower values compared to the water flow. This is especially seen for Reynolds numbers below $100\,000$ presented in Fig. 4. For Reynolds numbers above $100\,000$, the results of predictions using MDF and SDF are practically the same. Almost the same predictions of λ_m for $\mathrm{Re}_{ap} > 100\,000$ are due to the fact that the importance of dimensionless yield stress τ_0/τ_w decreases with the increasing wall shear stress.

Figure 4 demonstrates the gap between the predictions of friction factor for slurries with the yield stress $\tau_0 = (1.40\text{-}13.5)\,\mathrm{Pa}$ and $\tau_0 = 43\,\mathrm{Pa}$ if SDF and MDF are used. As it is seen in Fig. 4, the friction factor (MDF) for low and moderate yield stress, $\tau_0 = (1.40\text{-}13.5)\,\mathrm{Pa}$, is practically the same – data set from No. 1 to No. 4 in Table 1, and is much lower comparing to the water flow if $\mathrm{Re}_{ap} < 100\,000$. For the high yield stress $\tau_0 = 43\,\mathrm{Pa}$, λ_m is significantly higher than for $\tau_0 = (1.40\text{-}13.5)\,\mathrm{Pa}$, however it is still much lower comparing to the water flow if $\mathrm{Re}_{ap} < 100\,000$. It is difficult to interpret the differences between
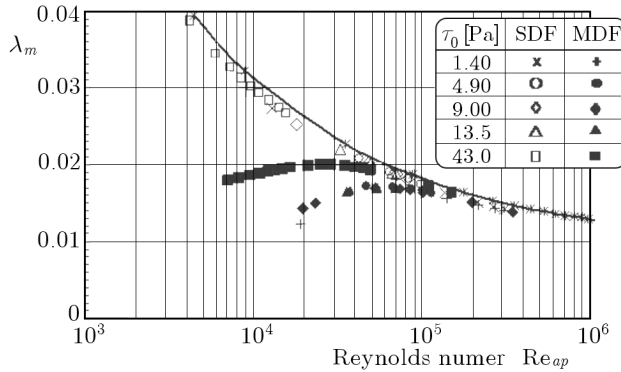
Fig. 4. Predictions of friction factor for turbulent flow of fine-dispersive slurry using standard (SDF) and modified turbulence damping function (MDF) and for water; data No. 1-5 in Table 1

predictions of λ_m for $\tau_0 = (1.4$-$13.5)$ Pa, and $\tau_0 = 43$ Pa (MDF). However, possible influence on that could be due to the level of turbulence intensity.
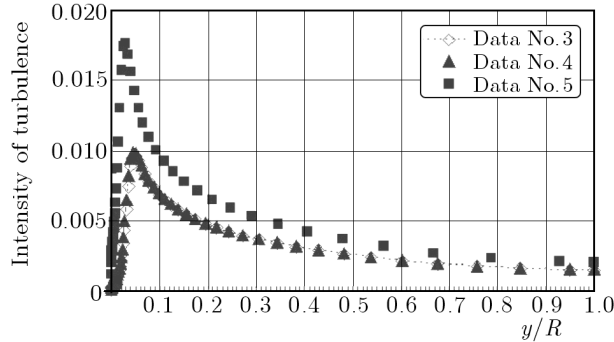

Fig. 5. Prediction of intensity of turbulence for slurry flow for moderate and high yield stress; data No. 3, 4 and 5 in Table 1

Figure 5 presents predictions of the intensity of turbulence defined by (4.3) for slurries with the yield stress equal to $\tau_0 = (9, 13.5, 43)$ Pa at the same value of Reynolds number defined by (4.2), which is $\mathrm{Re}_{ap} \approx 21000$ – data No. 3, 4 and 5 in Table 1. It is seen that the intensity of turbulence is practically the same if the yield stress is equal to 9 Pa or 13.5 Pa, while for $\tau_0 = 43$ Pa is

much higher. These could be a possible reason why the friction factor is the same for $\tau_0 = (1.40\text{-}13.5)\,\text{Pa}$ and much higher for $\tau_0 = 43\,\text{Pa}$

$$I = \frac{u'^2}{\overline{U}^2} \tag{4.3}$$

Analysing the results of predictions of the frictional head loss and friction factor for yield-stress slurries, one can say that both parameters substantially depend on the yield stress. All the aforementioned slurries exhibit significant decrease of turbulence as the friction factor is below that of the water flow.

5. Conclusions

Taking into account the mathematical model with the modified turbulence damping function and a proper rheological model allows predicting the frictional head loss and friction factor in a variety of fine-dispersive slurry flows. The turbulence damping function, which includes dimensionless yield stress, decreases the level of turbulence in the near wall region. The modified turbulence damping function approaches the standard Launder and Sharma one as the yield stress approaches zero. As a consequence of the introduced modified turbulence damping function, reduction of turbulence stress component $(-\rho u'v')$ at the wall takes place. The availability of the mathematical model together with an appropriate rheological model made it possible to design pipeline characteristics and optimization studies through numerical simulation.

Analysis of the frictional head loss and friction factor of fine-dispersive slurries with the yield stresses indicates that turbulence damping appears. This is coherent with the hypothesis proposed by Wilson and Thomas (1985) who reasoned that in slurry flows with fine solid particles the viscous sub-layer becomes thicker. It means that turbulence in the near-wall region is suppressed compared to a single-phase flow with the same flow conditions.

Significant decrease of turbulence near the pipe wall was demonstrated as the friction factor was below that for a water flow. This phenomenon is specially seen for Reynolds numbers up to $\text{Re}_{ap} \approx 100\,000$. For Reynolds numbers above $100\,000$, the friction factor is the same like for a Newtonian liquid flow. It was shown that the frictional head loss and the friction factor substantially depend on the yield stress.

Possible cause of turbulence damping near the pipe wall could result from the existence of lift forces. The existence of lift forces causes that bigger particles are pushed away from the pipe wall. As a result of diffusion processes,

bigger particles are replaced by smaller ones. Small particles are responsible for the increase of viscosity, which increases damping of turbulence fluctuation. This exists however, in close vicinity of the pipe wall in which the shear rate is high

$$R^+ = \frac{1}{\mu_{pl}}\Big[(R-r)\sqrt{\frac{\tau_w}{\rho_m}}\,\rho_m\Big(1-\frac{\tau_0}{\tau_w}\Big)\Big] \tag{5.1}$$

Recent analysis of Bartosik (2009), indicates that in a fine-dispersive slurry flow the viscous sublayer depends on the yield stress and can exceed $R^+ = 10$, described by Eq. (5.1), if the yield stress is sufficiently high, while in the case of Newtonian liquid flow it exists for $0 < R^+ \leqslant 5$.

References

1. Bartosik A., 1997, Modification of k-ε model for slurry flow with the yield stress, *Proc. 10th Int. Conf. Numerical Methods in Laminar and Turbulent Flow*, Pineridge Press, **10**, 265-274

2. Bartosik A., 2001, Measurements and predictions of velocity distribution in turbulent flow of Bingham hydromixture, *Chemical and Process Engineering*, **22**, 3B, 223-228

3. Bartosik A., 2004, Influence of rheological models on numerical prediction of turbulent flow, *Proc. 12th Inter. Symposium on Freight Pipelines*, Prague, September 2004, *Sc. Papers of the Agricultural Academy of Wrocław*, Editor: Academy of Sciences of the Czech Republic, **481**, 167-174

4. Bartosik A., 2006, Modelling of a turbulent flow using the Herschel-Bulkley rheological model, *Chemical and Processing Engineering*, **27**, 623-632

5. Bartosik A., 2008, Laminarisation effect in fine-dispersive slurry flow, *Archives of Thermodynamics*, **29**, 3, 69-82

6. Bartosik A., 2009, *Badania symulacyjne i eksperymentalne osiowo-symetrycznego przepływu drobno- i grubodyspersyjnej hydromieszaniny w przewodach tłocznych*, Monografia M11, Wyd. Politechniki Świętokrzyskiej, Kielce

7. Bartosik A., 2010, Application of rheological models in prediction of turbulent slurry flow, *Flow, Turbulence and Combustion*, Springer-Verlag, **84**, 2, 277-293

8. Bartosik A., Hill K., Shook C., 1997, Numerical modelling of turbulent Bingham flow, *9th Int. Conf. Transport and Sedimentation of Solid Particles*, Kraków September'97, *Sc. Papers of the Agricultural University of Wrocław*, **315**, Part 1, 69-81

9. Chen R.C., Kadambi J.R., 1995, Discrimination between solid and liquid velocities in slurry flow using Doppler Velocimeter, *ASME, Powder Technology*, **85**, 127-134

10. Cui H., Grace J.R., 2007, Flow of pulp fibre suspension and slurries: A review, *International J. Multiphase Flow*, **33**, 921-934

11. Danon H., Wolfshtein M., Hetsroni G., 1977, Numerical calculations of two phase turbulent round jet, *Int. J. Multiphase Flow*, **3**, 223-234

12. Doron P., Barnea D., 1996, Flow pattern maps for solid liquid flow in pipes, *Int. J. Multiphase Flow*, **22**, 273-283

13. Hinze J.O., 1971, Turbulent fluid and particle interaction, *Prog. Heat Mass Transfer*, **6**, 433-452

14. Kuboi R., Komasawa I., Otake T., 1974, Fluid and particle motion in turbulent dispersion – II – influence of turbulence of liquid on the motion of suspended particles, *Chem. Eng. Sci.*, **29**, 651-657

15. Launder B.E., Sharma B.I., 1974, Application of the energy-dissipation model of turbulence to the calculation of flow near a spinning disc, *Letters in Heat and Mass Transfer*, **1**, 131-138

16. Li Y., Zhou L.X., 1996, A k-ε-PDF two-phase turbulence model for simulating sudden-expansion particle-laden flows, *Proc. ASME Fluids Engineering Division Summer Meeting*, July 7-11, 1996, San Diego, CA, 1, 311-315

17. Ling J., Skudarnov P.V., Lin C.X., Ebadian M.A., 2003, Numerical investigations of liquid-solid slurry flows in a fully developed turbulent flow region, *Int. J. Heat and Fluid Flow*, **24**, 389-398

18. Mishra R., Singh S.N., Seshadri V., 1998, Improved model for the prediction of pressure drop and velocity field in multi-sized particulate slurry flow through horizontal pipes, *Powder Handling Processing*, **10**, 3, 279-287

19. Nouri J.M., Whitelaw J.H., 1992, Particle velocity characteristics of dilute to moderately dense suspension flows in stirred reactors, *Int. J. Multiphase Flow*, **18**, 1, 21-33

20. Roco M.C., Balakrishnan N., 1985, Multi-dimensional flow analysis of solid-liquid mixtures, *J. Rheology*, **29**, 4, 431-456

21. Roco M.C., Shook C.A., 1983, Modelling of slurry flow: the effect of particle size, *Can. J. Chem. Engng.*, **61**, 494-503

22. Schreck S., Kleis S.J., 1993, Modification of grid-generated turbulence by solid particles, *J. Fluid Mech.*, **249**, 665-688

23. Shook C.A., Roco M.C., 1991, *Slurry Flow: Principles and Practice*, Butterworth-Heinemann, Boston

24. Slatter P.T., 1994, *Transitional and Turbulent Flow of Non-Newtonian Slurries in Pipes*, PhD Thesis, University of Cape Town

25. Slatter P.T., Wasp E.J., 2000, The laminar/turbulent transition in large pipes, *Proc. 10th Int. Conf. Transport and Sedimentation of Solid Particles*, **2**, 389-399

26. Soo S.L., 1990, *Multiphase Fluid Dynamics*, Science Press, Beijing

27. Stainsby R., Chilton R.A., 1994, Prediction of the headlosses in non-Newtonian sludge pipelines using CFD, *Proc. 2nd CFDS Int. User Conf.*, Pittsburgh, 259-272

28. Stainsby R., Chilton R.A., 1996, Prediction of pressure losses in turbulent non-Newtonian flows: development and application of a hybrid rheological model, *Proc. BHR Group, Hydrotransport*, **13**, 21-39

29. Sundaresan S., Eaton J., Koch D.L., Ottino J.M., 2003, Appendix 2: Report of study group on disperse flow, *Int. J. Multiphase Flow*, **29**, 1069-1087

30. Wilson K.C., Thomas A.D., 1985, A new analysis of the turbulent flow of non-Newtonian fluids, *Can. J. Chem. Eng.*, **63**, 539-546

31. Wu Y., 1996, Computation on turbulent dilute liquid-particle flows through a centrifugal impeller by using the k-ε-Ap turbulence model, American Society of Mechanical Engineers, Fluids Engineering Division, *Proceed. ASME Fluids Engineering Division Summer Meeting*, Part 1, July 7-11, 1996, San Diego, CA, USA, 265-270

32. Yulin W.U., 1996, Computation of turbulent dilute liquid-particle flows through a centrifugal impeller by using the k-ε-Ap turbulence model, *Fluid Engineering Division Conference, FED, ASME*, **236**, 265-270

Symulacja strat tarcia w przepływie szlamu z progiem płynięcia, w którym występuje tłumienie turbulencji

Streszczenie

Artykuł dotyczy matematycznego modelowania w pełni rozwiniętego przepływu hydromieszaniny Binghama w przewodzie kołowym. Model matematyczny zbudowano na bazie równań Naviera-Stokesa z zastosowaniem koncepcji lepkości pozornej. Problem domknięcia układu równań, wynikający z dodatkowych składowych tensora naprężeń turbulentnych, rozwiązano poprzez użycie dwu równaniowego modelu turbulencji, w którym zastosowano zmodyfikowaną funkcję tłumiącą turbulencję przy ścianie. Ostateczna postać modelu matematycznego zawiera trzy nieliniowe równania różniczkowe cząstkowe. Głównym celem pracy jest przedstawienie wzmożonego tłumienia turbulencji w obszarze przyściennym, jako że współczynnik strat tarcia hydromieszaniny jest niższy w stosunku do wody. Artykuł przedstawia wyniki numerycznej

symulacji współczynnika strat tarcia dla szlamu z niskim, umiarkowanym i wysokim progiem płynięcia. Obliczony jednostkowy spadek ciśnienia porównano z wynikami badań eksperymentalnych, uzyskując satysfakcjonującą dokładność. Wykazano, że jednostkowy spadek ciśnienia i współczynnik strat tarcia zależą istotnie od progu płynięcia. Wyniki numerycznej symulacji przedstawiono w postaci wykresów i wniosków oraz omówiono możliwe przyczyny wzmożonego zjawiska tłumienia turbulencji przy ścianie.